Biomed Microdevices (2015) 17: 119
DOI 10.1007/s10544-015-0022-2

PicoMolar level detection of protein biomarkers based on electronic sizing of bead aggregates: theoretical and experimental considerations

Z. Lin[1] · X. Cao[1] · P. Xie[1] · M. Liu[1] · Mehdi Javanmard[1]

Published online: 21 November 2015

Abstract We demonstrate a novel method for electronically detecting and quantifying protein biomarkers using microfluidic impedance cytometry. Our biosensor, which consists of gold electrodes micro-fabricated in a microchannel, detects the differences between bead aggregates of varying sizes in a micro-pore sandwiched between two micro channels. We perform a sandwich immunoassay, where the complementary antibody pairs are immobilized on two different bead types, and the presence of antigen results in bead aggregation, the amount of which depends on antigen quantity. When single beads or bead aggregates pass through the impedance sensor, differences in impedance change are detected. In this manuscript, we perform a comprehensive theoretical study on the limits imposed on sensitivity of this technique due to electronic noise and also mass transfer and reaction limits. We also experimentally characterize the performance of this technique by validating the technique on an IgG detection assay. A detection limit at the picoMolar level is demonstrated, thus comparable in sensitivity to a sandwich ELISA.

Keywords Protein biomarker detection · Microfluidics · Impedance Cytometry

1 Introduction

The state of various diseases, both chronic and infectious, can be signaled by monitoring changes in concentrations of panels of protein biomarkers (Liao et al. 2004; Senolt et al. 2007; Uchida et al. 2002). For example, in the case of inflammatory diseases like asthma and rheumatoid arthritis, often an elevation of pro-inflammatory cytokine levels and a decrease in anti-inflammatory cytokines is observed (Verrills et al. 2011). To be able to effectively diagnose these diseases, monitor treatment, and better manage these conditions, there is a need for rapid, lightweight, and inexpensive tests for measuring protein concentrations in minute volumes of biological samples such as blood, sweat, urine, and even exhaled breath condensate. However, this kind of assay is currently performed using bulky instruments based on optical technologies like sandwich ELISA or protein microarrays, methods which are expensive and require sending the samples out to a centralized laboratory to perform the tests. As a result, lightweight, portable, high accuracy and highly sensitive protein analyzers low in cost are urgently needed to enable point-of-care and even home testing.

The gold standard method for protein detection and quantification is the sandwich ELISA technique, based on fluorescence detection, with an assay time of at least 1 h, a detection limit on the order of 1 pM, and a dynamic range of 2 to 3 orders of magnitude (Lequin 2005). Fluorescent plate readers are generally large and bulky and costly. Miniaturization of this type of assay can be accomplished by either performing the detection electronically, (Emaminejad et al. 2012; Javanmard et al. 2009; Mok et al. 2014) or by scaling down the size of the optical instrumentation, for example by using cameras on mobile phones (Tseng et al. 2010; Isikman et al. 2011, 2012a, b; Bishara et al. 2010, 2012; Su et al. 2010; Mudanyali et al. 2011; Ozcan 2010; Greenbaum and Ozcan 2012). We present a novel electronic detection technique for assaying proteins at the picoMolar level. We also discuss the theoretical considerations for the detection limit in terms of noise and also mass transfer and reaction processes.

✉ Mehdi Javanmard
mehdi.javanmard@rutgers.edu

[1] Rutgers, The State University Of New Jersey, Piscataway, NJ 08854, USA

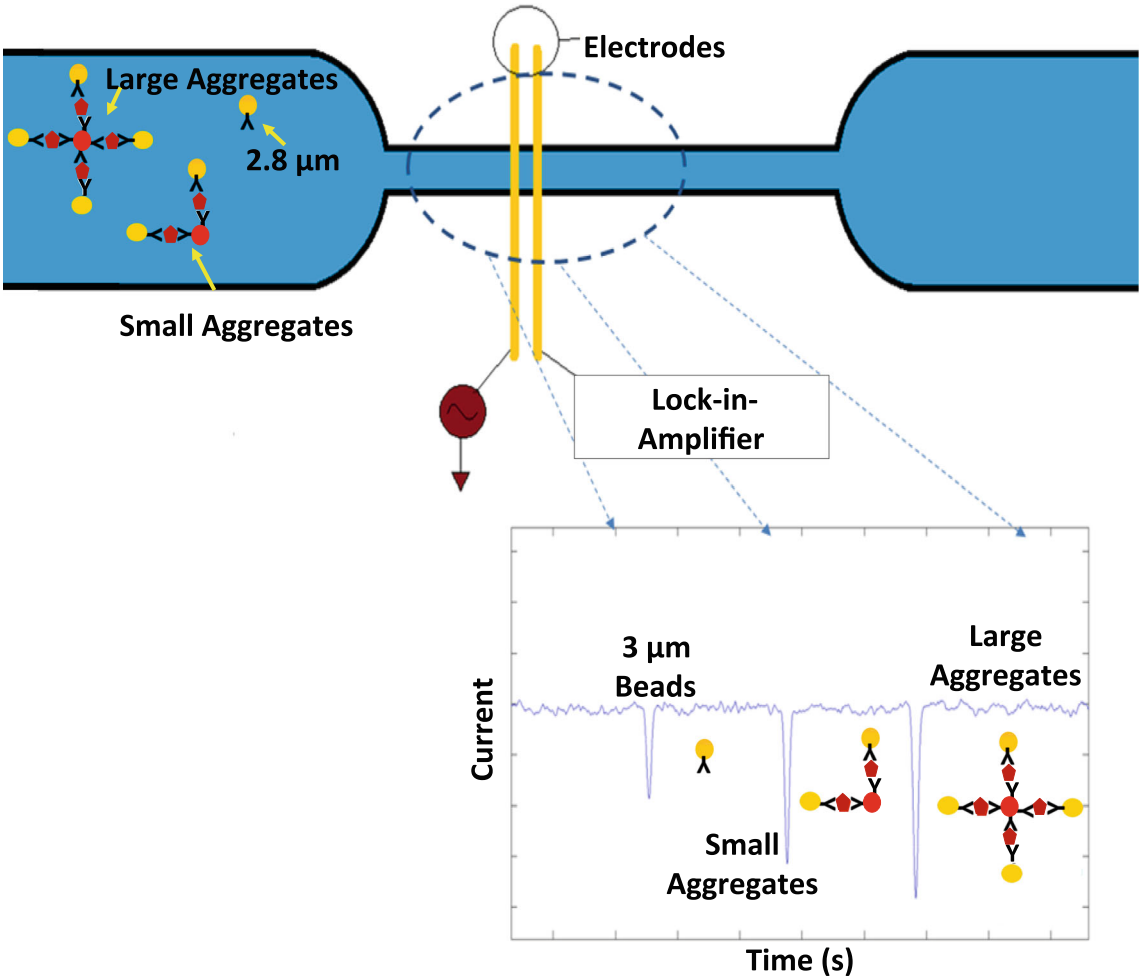

Fig. 1 Schematic of biochip. Presence of target protein results in beads with complementary antibody pairs to bind together and aggregate. Impedance based sizing allows differentiation between unbound beads and bead aggregates. The proportion of bead aggregates compared to the total bead count is used to quantify protein

Figure 1 shows the basic device. The detection concept is based on binding beads together and measuring the change in the size of the bead aggregate. The assay works by immobilizing two different bead types with complementary antibody pairs. One bead type is magnetic and the other non-magnetic. The target antigen is mixed with the magnetic beads. The polystyrene beads are then added to the mix allowing the antibody pairs to form a sandwich immunocomplex, thus aggregating the beads together. Then a magnet is used to separate the unbound polystyrene beads from the mixed soup, thus simplifying the downstream quantification. The presence of the target antigen, depending on its quantity, results in varying levels of bead aggregation. An impedance cytometer is then used to size the bead aggregates and estimate the protein quantity. The result is a mixed soup

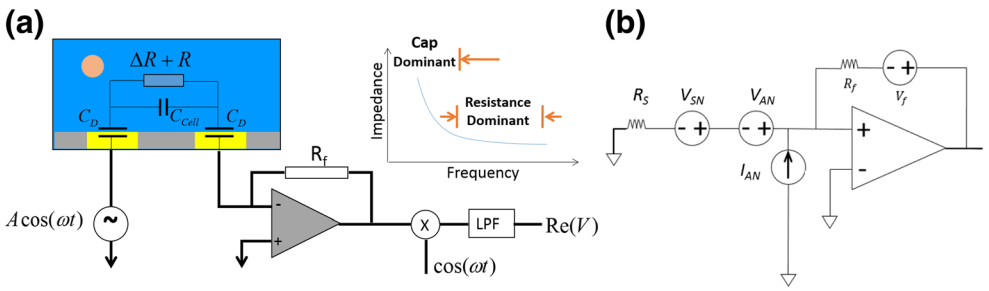

Fig. 2 (**a**) Equivalent circuit model of the electrode-electrolyte interface in the microchannel along with the readout circuit for measuring changes in resistance across the channel. (**b**) The equivalent noise circuit model shows the various sources contributing to the noise of the circuit

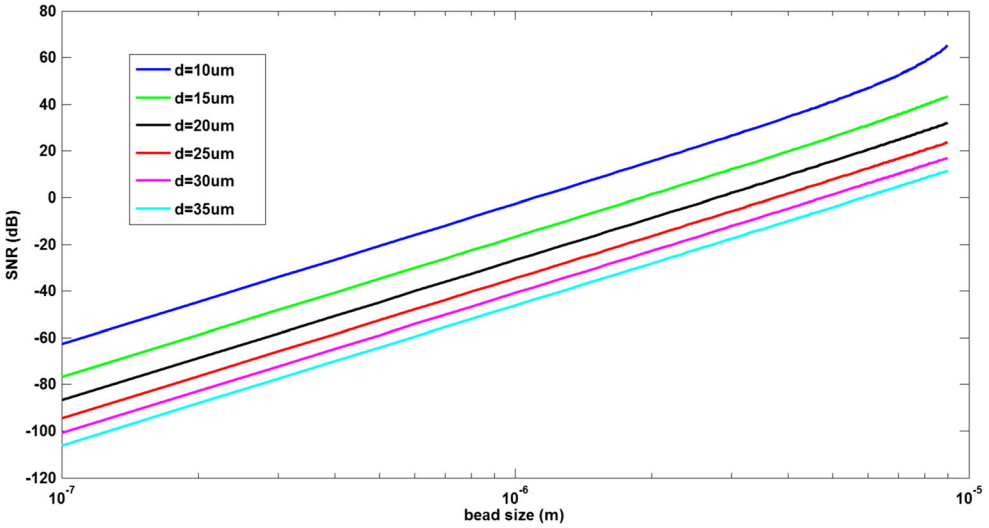

Fig. 3 Signal to noise ratio of beads of various sizes inside a microfluidic channel of varying dimensions

of aggregated magnetic-polystyrene bead complexes, non-aggregated magnetic beads and non-aggregated polystyrene beads. The amplitude distribution of the acquired peaks corresponds to the particle size distribution, based on which varying quantities of proteins can be detected.

1.1 Theory

In this section we discuss the theoretical considerations in determining the performance limit of the sensing system both electronically and in terms of mass transfer and reaction limitations. In our design, we assume an ideal polarizable electrode system without any faradaic reactions since we use gold as our electrode material. Application of a voltage across the two electrodes results in a double layer of ions with opposing polarity forming a boundary and acting as a capacitance, which is commonly referred to as the double-layer capacitance. Thus we use a simplified circuit model (Fig. 2a) with a double layer capacitance (C_{dl}) at each electrode in series with the solution resistance (R_s) all in parallel with the coupling capacitance between the two electrodes in the cell (C_{cell}).

The equivalent impedance of this model is calculated with two capacitors C_{dl} in series with a resistor R_s, in parallel with a capacitor and resistor C_{cell}, which is shown below

$$Z = \left(\frac{2}{j\omega C_{dl}} + R_S\right) \| C_{cell} = \frac{2 + R_S C_{dl} j\omega}{2C_{cell} j\omega - C_{dl} R_S C_{Cell} \omega^2 + C_{dl} j\omega} \quad (1)$$

We obtain the poles and zeros from Eq. (1), $f_{pole1} = 0, f_{pole2} = \frac{2C_{cell}+C_{dl}}{2\pi R_S C_{cell} C_{dl}}, f_{zero} = \frac{1}{\pi R_S C_{dl}}$.

The region between f_{pole1} and f_{pole2}, the system is purely resistive. Thus, we operate within this frequency range so that our response is primarily resistive to measure the changes in resistance as the beads transit across the electrode pair.

1.1.1 Noise calculation

By operating at within the frequency range between f_{pole1} and f_{pole2} in our system, the resistance is simplified to R_s, thus allowing us to model our equivalent noise circuit as (Fig. 2b). Here we make the assumption that the noise of the mixer and low pass filter is significantly smaller than the trans-impedance amplifier noise.

The input referred current noise of the system can be described as follows:

$$I_{in}^2 = I_{AN}^2 + \frac{V_{SN}^2}{{R_S}^2} + \frac{V_{AN}^2}{{R_S}^2} + \frac{V_f^2}{{R_f}^2} \quad (2)$$

We use R_s=200$k\Omega$ R_f=1$k\Omega$, R_f=1$k\Omega$, C_{dl}=1nF, and C_{cell}=1pF and we obtain f_{zero}=79.6kHz and f_{pole2}=39.9MHz, $V_R^2 = 4kTR_S = 3.314 \times 10^{-15} V^2/Hz$, and $V_f^2 = 4kTR_f = 1.657 \times 10^{-17} V^2/Hz$. For measurements,

Table 1 Relationship between detection limit and percentage of non-specifically bound beads

Non-Specific Bead Binding Percentage	0.01 %	0.1 %	1.0 %
Detection Limit	100 fM	1 pM	10 pM

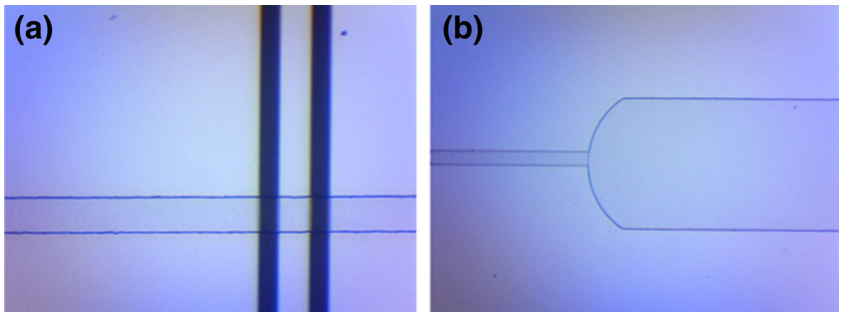

Fig. 4 Microscopic images of fabricated device (**a**) Electrodes integrated in the micropore (**b**) The entrance of the 300 μm channel tapering down to the 30 μm wide pore

we used 300 kHz as our operating frequency, which is between f_{zero} and f_{pole2}.

For the lock-in amplifier, we assume a current noise of $1pA/\sqrt{Hz}$ and a voltage noise of $6nV/\sqrt{Hz}$, and we ignore the noise from the mixer and low pass filter, because it is negligible compared to the input current and voltage noise of the amplifier. Because we use a low pass filter bandwidth of 100 Hz, the input current noise comes to approximately 42 pA. The change in impedance as each bead passes through electrodes is (Deblois and Bean 1970)

$$\Delta R = 2\rho_{sol}\left(\frac{\tan^{-1}\left(\frac{d}{2\sqrt{\frac{A_c}{\pi}-\frac{d^2}{4}}}\right)}{\pi\sqrt{\frac{A_c}{\pi}-\frac{d^2}{4}}}-\frac{d}{2A_c}\right) \tag{3}$$

where $A_c=h\times l$, the height and width of our pore is 10 μm× 30 μm, assuming a solution resistivity of 1.176 Ω/m (PBS).

The change in signal amplitude resulting from a passing particle is equal to:

$$\Delta I(j\omega) = \frac{\Delta R}{R^2}\left(\frac{\omega^2}{\omega^2+\left(\frac{2}{RC_{dl}}\right)^2}\right)V_{in}\approx\frac{1}{R}\frac{\Delta R}{R}V_{in} \tag{4}$$

We use the calculation of ΔI and I_{in} to calculate the signal to noise ratio based on bead diameter and pore dimensions, as shown in Fig. 3. Our theory predicts that we can comfortably detect 3 μm particles at the single bead level.

1.1.2 Detection limit and capture rate

Given that the primary antibody coated beads are mixed with the target antigen continuously in solution, we assume that we are operating in a regime with 100 % efficient mixing, and thus we are reaction limited rather than mass transport limited (Squires et al. 2008). The antigen capture rate (C_a) in this case can be estimated by using the first order Langmuir equation,

$$C_a = {}^{b(t)}/_{b_m} = \frac{C_o/K_D}{1+C_o/K_D} \tag{5}$$

where $b(t)$ is the concentration of the bound receptors on the surface of the beads, b_m is the concentration of total receptors on the surface of the beads, and C_o is the concentration of antigen in solution, and K_D is the dissociation constant of the antigen antibody interaction. Often from experimental experience, we find that sensitivity is limited by non-specific binding. Varying percentages of nonspecific bead capture, will result in larger detection limit as shown in Table 1.

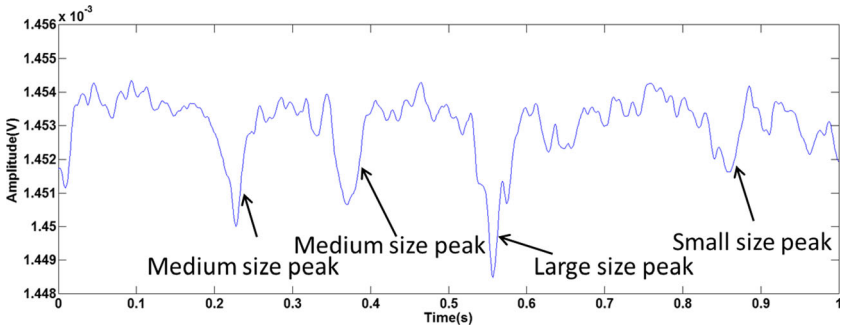

Fig. 5 Representative data of output voltage trace verses time for varying sizes of bead aggregates including single beads, medium sized aggregates, and larger aggregates

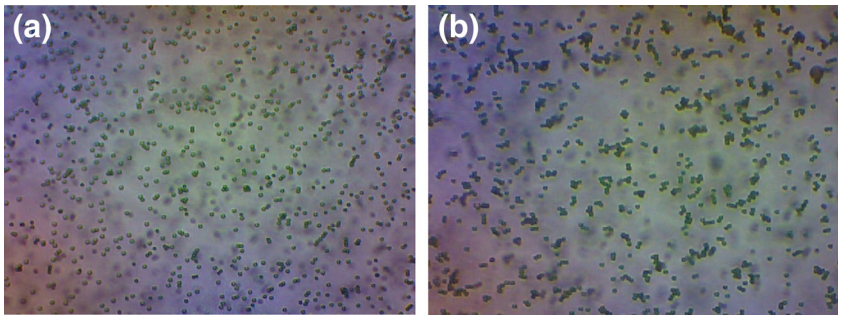

Fig. 6 Microscopic image of (**a**) negative control experiment with no IgG present resulting in very little bead aggregation. (**b**) positive experiment where presence of IgG results in aggregation of beads

2 Materials and methods

The fabricated micro-channel is 300 μm wide and 30 μm in height and tapers down to a 30 μm wide and 10 μm high micro-pore, to allow for sensitivity at the single bead level for 3 μm beads. Shown in Fig. 4a and b are microscopic images of the micro fabricated devices. The width of each electrode is 20 μm while the space between each two electrodes is 25 μm. To fabricate the electrodes, we perform standard photolithography on a 3″ fused silica wafer. We photo-pattern the resist on the fused silica wafer, and then we perform electron beam metal evaporation and liftoff. We choose gold as our electrode material due to its inert nature and resistance against corrosion. For photo-patterning we clean the wafer, spin coat the photoresist, soft bake the resist, expose the photoresist with ultra-violet light through a 4″×4″ chromium mask, develop the resist, and finally hard bake the resist. After photo-patterning, we deposit a 100 nm gold layer using electron beam evaporation. We use a 10 nm layer of chromium for enhanced adhesion of gold to glass, otherwise the gold film often gets removed during liftoff.

2.1 Microfluidic channel fabrication

We fabricate the microfluidic channel (30 μm wide and 10 μm high) in PDMS (Polydimethyl Siloxane using soft lithography. To fabricate the master mold of the channel, we photopatterned a layer of SU-8 onto a 3″ Silicon wafer. The patterning of SU-8 involves standard photolithography which includes cleaning of the silicon wafer, spin coating the photoresist, soft baking the resist, exposure of UV light to the resist, development of the resist, and hard bake of the SU-8. We then pour PDMS (10:1 pre-polymer/ curing agent) onto the master mold and cured the PDMS by baking the wafer at 80 °C for 2 h. After curing the PDMS chip, we peeled it off from the mold. We then punched a 1.5 mm hole and a 5 mm hole forming the inlet and outlet respectively. We then align the PDMS substrate and bonded it to the electrode chip after both substrates have undergone oxygen plasma treatment. After bonding the two chips together, we baked them at 60 °C for 30 min to form the irreversible bond.

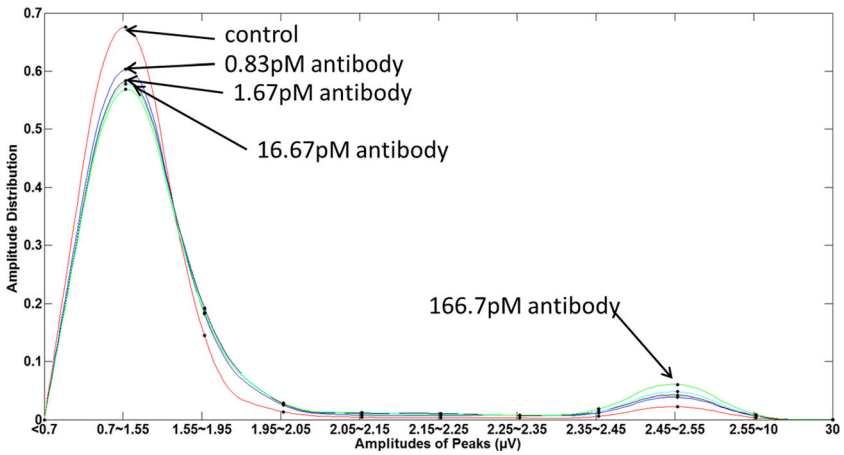

Fig. 7 Normalized amplitude distribution for various concentrations of IgG ranging from 166 pM to 0 pM. For all concentrations, two peaks are observed in the distribution. The first peak results from unaggregated beads in the mixture, and the second peak which is at higher amplitudes results from bead aggregates. As IgG concentration increases, the second peak becomes larger in size, whereas the first peak decreases in size. Detection of IgG is achieved at ~1 pM level which is comparable to an ELISA

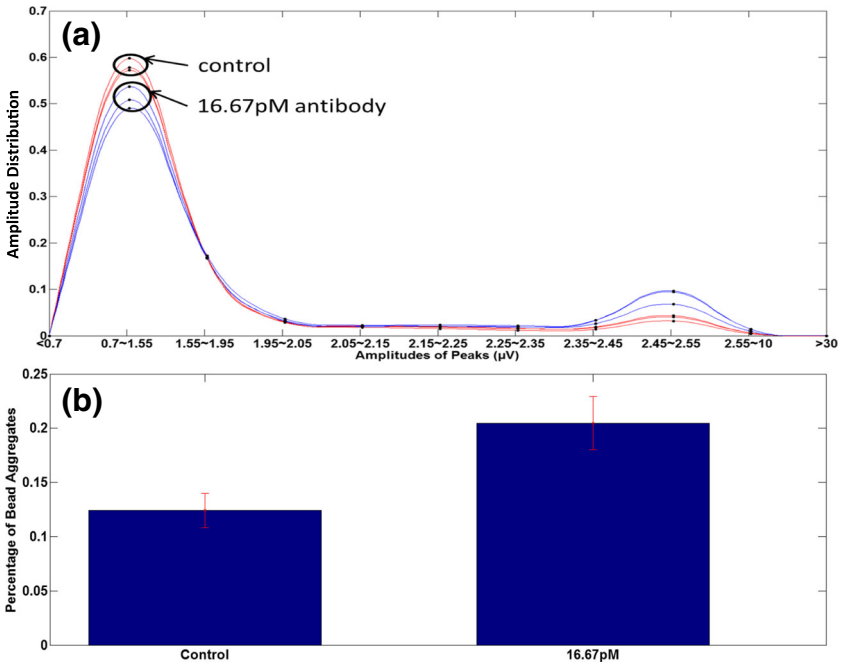

Fig. 8 Assay is performed in triplicate for concentration of 16.667 pM to validate assay repeatability as shown in the (**a**) amplitude distribution plot, and also (**b**) the ratio of the integral under the second peak (corresponding to bead aggregates) with respect to the first peak (corresponding to unaggregated beads)

2.1.1 Bead assay

To demonstrate proof-of-concept and characterize the detection limit of our technique, we perform an IgG detection assay. We use two different bead types coated with anti-mouse IgG antibodies for capture and subsequent quantification of mouse IgG antibodies. We used 3 μm polystyrene beads (Spherotech, Lake Forest, IL) coated with anti-mouse IgG antibodies, and also 2.8 μm paramagnetic Dynal beads (Life Technologies, Carlsbad, CA) coated with anti-mouse IgG antibodies. The protocol for performing the assay went as follows: Sheep anti-mouse IgG beads were washed three times with PBS 0.1 % BSA. Mouse IgG antibody suspended in PBS (Phosphate Buffer Saline) was added into the to the epindorph tube, thus resuspending the beads. The beads were mixed and rotated for 1 h to ensure capture of the mouse IgG antibodies. The beads were again washed three times with PBS 0.1 % BSA. Afterwards, 3 μm polystyrene beads were added into the epindorph tube, and rotated for 2 h to ensure that there was sufficient time to bind together. A magnetic field was then applied to separate the magnetic beads and the polystyrene beads bound to magnetic beads from the unbound polystyrene beads. This was repeated several times to ensure that the unbound polystyrene beads are removed from the mixture. The assay was performed at multiple mouse IgG concentrations. The assay was validated both electronically and optically as explained below.

2.1.2 Measurement

The microfluidic chip was connected to a lock-in amplifier (Zurich Instrument HF2 series) through two wire-bonding pads tied to the electrodes. The frequency and amplitude of the input AC voltage are 300 kHz and 1 V peak-to-peak. We applied a gain of 1 kV/amp to the transimpedance amplifier. In order to confirm that the peaks were indeed due to beads passing across the sensor, we simultaneously monitored the microchannel under an optical microscope while monitoring the impedance. The recorded data was then processed using a custom-written code in Matlab, which performed detrending and denoising of the data, and subsequent peak counting and determination of the amplitude distribution of the peaks to distinguish single beads from bead aggregates (Fig. 5).

3 Results and discussion

We performed experiments with a multitude of IgG concentrations to demonstrate sensitivity and repeatability of our sensing approach. Figure 6 shows optical images comparing beads which have aggregated due to IgG binding with anti-IgG on the beads compared to the negative control assay where IgG was not present. The images confirm that bead aggregation occurs. Figure 5 shows representative data of voltage traces as a function of time. Bead aggregates result in larger peaks compared to non-aggregated beads. We also show peak size distribution (Fig. 7) of the beads for various concentrations, demonstrating detection all the way down to the picoMolar level. Based on the plotted distribution of peak amplitude, we found that the most reliable method for protein quantification can be found based on taking

the ratio of the integral of all amplitudes greater than 2 μV with respect to the integral of the amplitude of all peaks less than 2 μV. To demonstrate repeatability of the assay, we repeated the experiment at 16 pM and the negative control each at least three times. Figure 8a shows the amplitude distribution and Fig. 8b shows the ratio of the integral sum of all peaks greater than 2 μV and the integral sum of all peaks smaller than 2 μV including the error bars.

4 Summary and conclusions

In conclusion, we have designed, micro-fabricated, and validated a novel miniaturized assay for detection of proteins. Our experimental results show that bead aggregates result in larger change in comparison with non-aggregated beads, and that based on electronic bead aggregate sizing we are able to detect proteins down to the picoMolar, which is comparable to the gold standard ELISA method. We are also able to quantify the concentration of proteins. Although we focused on detection of IgG in this work, we emphasize that this approach is applicable to a broad range of proteins, as long as a high affinity antibody pair is available. Here we made use of a commercial lock-in-amplifier, however we can easily integrate the readout circuitry onto a miniaturized CMOS chip, significantly reducing the footprint of the system as a whole. Future work will focus on applying this tool to detecting panels of proteins in complex samples like blood, urine, and exhaled breath condensate.

References

W. Bishara, T.-W. Su, A.F. Coskun, A. Ozcan, Opt. Express **18**(11), 11181–11191 (2010)

W. Bishara, S.O. Isikman, A. Ozcan, Ann. Biomed. Eng. **40**(2), 251–262 (2012)

R. W. DeBlois, C. P. Bean, Rev. of Sci. Inst. **41**(7), 909–916 (1970)

S. Emaminejad, M. Javanmard, R.W. Dutton, R.W. Davis, Anal. Chem. **84**(24), 10793–10801 (2012)

A. Greenbaum, A. Ozcan, Opt. Express 3129 (2012)

S.O. Isikman, W. Bishara, A. Ozcan, Appl. Opt. H253 (2011)

S.O. Isikman, W. Bishara, O. Mudanyali, I. Sencan, T.W. Su, D.K. Tseng, O. Yaglidere, U. Sikora, A. Ozcan, IEEE J. Sel. Top. Quantum Electron. **18**(3), 1059–1072 (2012a)

S.O. Isikman, A. Greenbaum, W. Luo, A. F. Coskun, A. Ozcan, PLoS One 7(9) (2012)

M. Javanmard, A.H. Talasaz, M. Nemat-Gorgani, F. Pease, M. Ronaghi, R.W. Davis, Lab Chip **9**(10), 1429–1434 (2009b)

R.M. Lequin, Clin. Chem. **51**(12), 2415–2418 (2005)

H. Liao, J. Wu, E. Kuhn, W. Chin, B. Chang, M.D. Jones, S.O. Neil, K.R. Clauser, J. Karl, F. Hasler, R. Roubenoff, W. Zolg, B.C. Guild, S. O'Neil, Arthritis Rheum. **50**(12), 3792–3803 (2004)

J. Mok, M.N. Mindrinos, R.W. Davis, M. Javanmard, Proc. Natl. Acad. Sci. U. S. A. **111**, 2110–2115 (2014)

O. Mudanyali, W. Bishara, A. Ozcan, Opt. Express 17378 (2011)

A. Ozcan, SPIE Newsroom (2010)

L. Senolt, D. Housa, Z. Vernerová, T. Jirásek, R. Svobodová, D. Veigl, K. Anderlová, U. Müller-Ladner, K. Pavelka, M. Haluzík, Ann. Rheum. Dis. **66**(4), 458–463 (2007)

T.M. Squires, R.J. Messinger, S.R. Manalis, **26**(4), 417–426 (2008)

T.W. Su, A. Erlinger, D. Tseng, A. Ozcan, Anal. Chem. **82**(19), 8307–8312 (2010)

D. Tseng, O. Mudanyali, C. Oztoprak, S.O. Isikman, I. Sencan, O. Yaglidere, A. Ozcan, Lab Chip **10**(14), 1787–1792 (2010)

T. Uchida, A. Fukawa, M. Uchida, K. Fujita, K.J. Saito, Proteome Res. **1**(6), 495–499 (2002)

N.M. Verrills, J.A. Irwin, X.Y. He, L.G. Wood, H. Powell, J.L. Simpson, V.M. McDonald, A. Sim, P.G. Gibson, Am. J. Respir. Crit. Care Med. **183**(12), 1633–1643 (2011)